Pergamon

Geochimica et Cosmochimica Acta, Vol. 64, No. 6, pp. 997–1011, 2000

0016-7037/00 $20.00 + .00

PII S0016-7037(99)00380-4

High resolution distribution of trace elements in the calcite shell layer of modern *Mytilus edulis*: Environmental and biological controls

ERIKA VANDER PUTTEN,[1,*] FRANK DEHAIRS,[1] EDDY KEPPENS,[2] and WILLY BAEYENS[2]

[1]Faculteit Wetenschappen, Laboratorium voor Analytische Chemie, Vrije Universiteit Brussel, Pleinlaan 2, 1050 Brussel, Belgium
[2]Faculteit Wetenschappen, Laboratorium voor Geochronologie, Vrije Universiteit Brussel, Pleinlaan 2, 1050 Brussel, Belgium

(*Received April* 22, 1999; *accepted in revised form October* 14, 1999)

Abstract—Mussels of a similar size, originating from the same population, have been grown in the field and the high resolution distribution of Mg, Mn, Sr, Ba and Pb in their calcite shell layer, as determined by Laser Ablation-Inductively Coupled Plasma-Mass Spectrometry, has been compared to temporal variations of environmental parameters.

All elements exhibit cyclic variations with an annual periodicity. The Mg, Sr and Pb cycles show great similarity and are characterised by a broad maximum during spring and early summer. These profiles cannot be explained by seasonal variations in the seawater composition. Skeletal Mg covaries reproducibly with temperature during spring but this covariation is abruptly interrupted after the spring phytoplankton bloom. The absence of a constant Mg-temperature relationship over the year hampers the direct use of Mg in *M. edulis* calcite as a high resolution temperature proxy.

The sharp peak that is dominating each skeletal Ba cycle coincides with the annual algal biomass maximum and presumably reflects elevated concentrations of particulate Ba, associated with the spring phytoplankton bloom. Similarly, elevated skeletal Mn concentrations during spring might reflect bloom-induced increases in particulate Mn. Skeletal $\delta^{13}C$ shows a seasonal variation, characterised by a minimum that coincides with the Mn maximum. These $\delta^{13}C$ variations are not in equilibrium with the seasonal $\delta^{13}C$ trend of the seawater dissolved inorganic carbon and presumably reflect fluctuations in the contribution of metabolic carbon to the shell carbonate, corresponding to seasonal variations in the mussel's respiration rate. *Copyright © 2000 Elsevier Science Ltd*

1. INTRODUCTION

The element composition of mollusc shells has been shown to be related to environmental parameters (Dodd, 1965; Lorens and Bender, 1980; Bourgoin, 1990; Pitts and Wallace, 1994; Klein et al., 1996a,b). As a result, the successively deposited shell calcium carbonate layers are potential archives of the varying environmental conditions the mollusc has experienced during its life (e.g., Fuge et al., 1993; Klein et al., 1996a,b; Stecher et al., 1996; Hart and Blusztajn, 1998). Slow growing, long living animals could provide records of progressive environmental changes while fast growing animals could record recurrent seasonal variations of environmental parameters. Sensitive microanalysis techniques, such as Laser Ablation-Inductively Coupled Plasma-Mass Spectrometry (LA-ICP-MS; see Perkins and Pearce, 1995, for a review of this technique), offer the possibility to analyse these shell chemical archives at a high spatial and thus temporal resolution. This has already been demonstrated in a number of studies (Fuge et al., 1993; Raith et al., 1996; Schettler and Pearce, 1996; Stecher et al., 1996; Price and Pearce, 1997). One mollusc genus that could be particularly well suited for extracting (paleo)environmental information via shell analysis, is *Mytilus*: thanks to the high longitudinal growth rate of their calcite shell layer, combined with a wide geographic distribution (Gossling, 1992) and tolerance to a broad range of environmental conditions (Seed and Suchanek, 1992), these bivalves might provide high resolution records of a large variety of environments. The potential of *Mytilus trossulus* for paleoreconstruction has been illustrated by Klein et al. (1996a) who reported that the Mg/Ca variations within the calcite shell layer of this mollusc provide an accurate record of seasonally varying sea surface temperatures. Furthermore, *Mytilus* shells might provide an interesting alternative for soft tissue in the Mussel Watch programs that are conducted worldwide for the biomonitoring of heavy metal pollution (e.g., Beliaeff et al., 1997).

However, it is becoming increasingly clear that mollusc shell chemistry is also controlled by biological factors (Rosenberg and Hughes, 1991; Klein et al., 1996b), implying that the environmental records could be obscured by ontogenetic trends as well as by seasonal variations in the animals' physiology. The complex nature of the relationships between environmental and biological controls has been illustrated by Klein et al. (1996b). These authors proposed a model that integrates salinity and metabolic rate to explain the variability of Sr/Ca and $^{13}C/^{12}C$ in shells of *M. trossulus*. Therefore, although mollusc shells in general, and *Mytilus* shells in particular, might be powerful tools for the reconstruction and monitoring of (paleo) environmental conditions, a better insight into the different factors controlling shell chemistry is required for a correct interpretation of the element profiles. Furthermore, an evaluation of the variability of shell element chemistry between individuals is of utmost importance for establishing the precision on any environmental information inferred from shell composition. Insight into the factors governing skeletal element incorporation can be obtained by relating the element distribution within modern shells to the corresponding environmental

*Author to whom correspondence should be addressed (evderput@vub.ac.be).

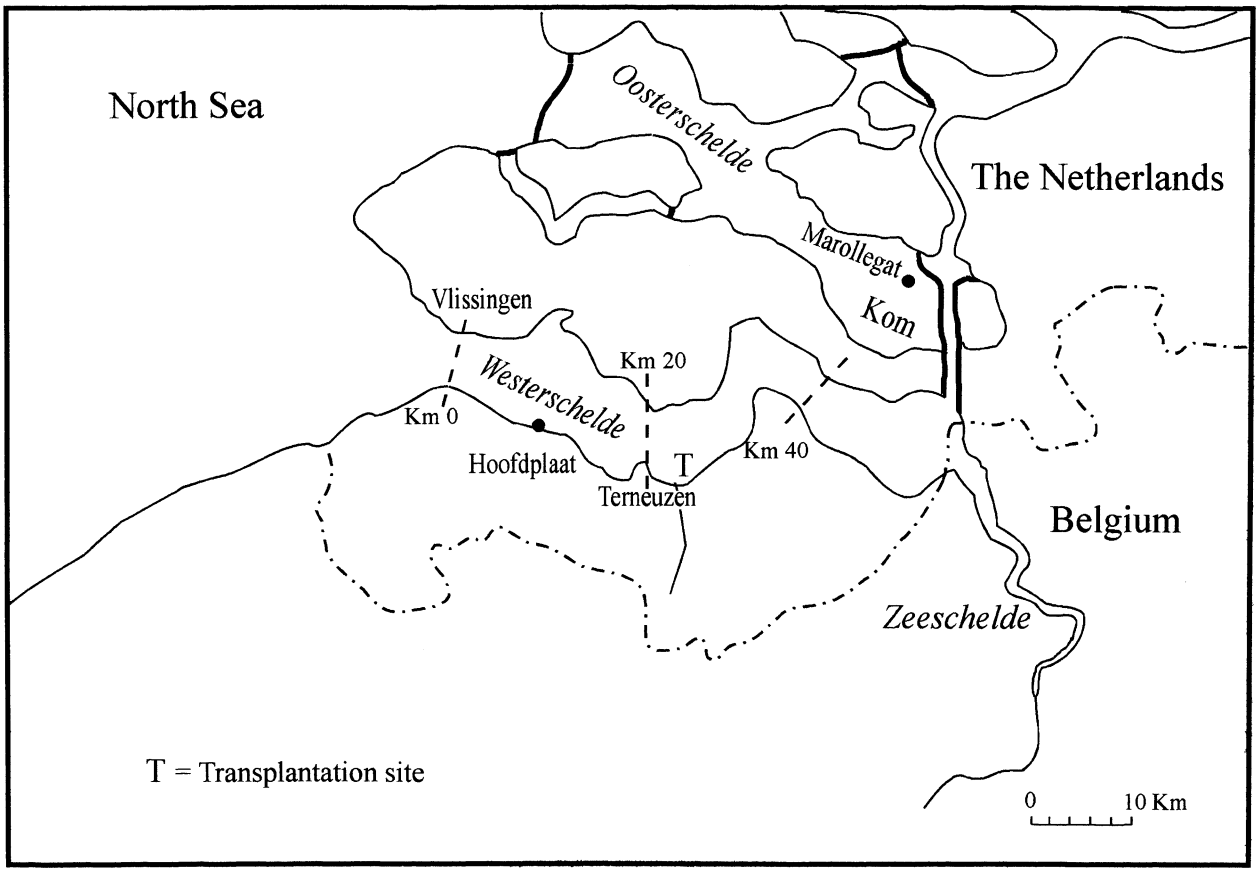

Fig. 1. Map of the Oosterschelde and Schelde estuary.

variations and biological cycles. For this purpose, shell stable isotope profiles can be of great value. Mollusc shell $\delta^{18}O$ has been shown to be influenced only by temperature and salinity (e.g., Epstein et al., 1953) and can thus provide information on the seasonality of shell chemistry. Mollusc shell $\delta^{13}C$ has been shown to be related to environmental parameters (Mook, 1971; Donner and Nord, 1986; Klein et al., 1996b) as well as to the animal's biology (Tanaka et al., 1986; Klein et al., 1996b) and could in this respect provide additional clues for interpretation of the shell element profiles.

In the present study, a field experiment with *M. edulis* has been combined with a high resolution LA-ICP-MS analysis of shell chemistry. The purpose of this approach was to get more insight into the processes controlling the incorporation of Mg, Mn, Sr, Ba, and Pb in the calcite shell layer of this bivalve. Mussels with a similar, accurately known shell length, originating from the same marine population, were transplanted to 3 locations along an estuarine gradient. On several occasions over a period of 14 months, a number of these transplanted mussels were collected and the element distribution patterns within their shells were compared to spatiotemporal environmental variations. First, the high resolution element profiles were compared to the corresponding temporal variations of several environmental parameters. For shell formed after transplantation, the seasonality of the skeletal element profiles was identified through the regular sampling of mussels during the transplantation period. For shell formed before transplantation, seasonality was identified by means of skeletal $\delta^{18}O$ analysis. Furthermore, differences in shell chemistry between individuals grown at different transplantation sites were evaluated in terms of spatial environmental differences. Since the mussels at each of these sites originated from the same population, variability due to potential (genetic) inter-population differences was eliminated. The present paper deals with the shell chemistry of mussels grown in one of the transplantation locations.

2. EXPERIMENTAL

2.1. Field Experiment

Mussels of 30 ± 1 mm were collected from a population in the Kom of the Oosterschelde (OS, The Netherlands; Fig. 1). The OS used to be a turbid estuary but has been transformed into a sheltered tidal bay as a result of the isolation of the estuary from river inputs and the construction of a storm-surge barrier (Nienhuis and Smaal, 1994). On April 20th, 1996, the mussels were caged and suspended in the intertidal zone of the marine part of the Schelde estuary (i.e., the Westerschelde—WS, The Netherlands) at a location just upstream from Terneuzen (Fig. 1). For a general description of the Schelde estuary, we refer to Baeyens et al. (1998b). Over a period of 14 months, a number of caged mussels were collected on several occasions for analysis of their shell chemistry. For 4 shells, collected on 06/30/96, 3 shells collected on 09/15/96, and 1 shell collected on each of the next 3 samplings, more specifically 11/27/96, 02/22/97 and 06/21/97, the distribution of Mg, Mn, Sr, Ba, and Pb was determined by Laser Ablation-Inductively Coupled Plasma-Mass Spectrometry (LA-ICP-

Table 1. Ranges of Laser Probe-ICP–MS operating conditions.

LaserProbe	
Laser mode	Q-switched
Flashlamp voltage	630–650 V
Laser output power	3–4 mJ/pulse
Repetition rate	4 Hz
Focus condition	focus
Preablation time	25 s
ICP—MS	
Forward power	1350 W
Reflected power	0 W
Argon flow rate	
carrier gas	1.1–1.21 min^{-1}
auxiliary gas	1.4–1.51 min^{-1}
cooling gas	13.51 min^{-1}
Acquisition mode	peak jumping
Points/peak	3
Dwell time	10.24 ms
Detector mode	pulse count
Acquisition time	20s

MS). For two mussels, one collected on 06/30/96 and another on 06/21/97, the shell $\delta^{18}O$ and $\delta^{13}C$ profiles were determined by mass spectrometric analysis.

2.2. Environmental Data

Temperature and salinity data for Marollegat, a site close to where the mussels were collected for transplantation, and for Hoofdplaat, a location 11 km downstream from the WS transplantation site (Fig. 1), were obtained from the Hydrometeostation of the «Ministerie van Verkeer en Waterstaat, Directoraat-Generaal Rijkswaterstaat, Directie Zeeland», The Netherlands. These parameters were recorded every 10 min. near the surface. The values used in the present study are averages over 24 h. Chlorophyll *a* concentrations (algal biomass measure) for Yerseke, a site close to where the mussels were collected for transplantation, and Vlissingen, a location approximately 18 km downstream from the WS transplantation site (Fig. 1), were obtained from the MWTL monitoring programs of the «Ministerie van Verkeer en Waterstaat, Directoraat-Generaal Rijkswaterstaat, Rijksinstituut voor Kust en Zee (RIKZ)», The Netherlands. Dissolved and particulate Pb-concentrations for Terneuzen, near the WS transplantation site (Fig. 1), were determined in the framework of the Joint Assessment and Monitoring Program of the Oslo-Paris Commissions (Koen Parmentier, personal communication).

2.3. Analysis of Shell Chemistry

The mussels were killed by steam and the soft tissue was separated from the shell. The shells were rinsed with milliQ water and dried for 48 h at 60°C. For LA-ICP-MS analysis, the shells were sectioned along the axis of maximal growth using a diamond saw. These sections were then polished with silicon carbide paper of decreasing grain size to visualise the boundary between the calcite and aragonite layer.

2.3.1. Determination of trace element profiles by means of LA-ICP-MS

For LA-ICP-MS analysis, a Fisons-VG PQII+ICP mass spectrometer and a Fisons-VG LaserProbe were used. The LaserProbe is based on a Spectron 150 mJ Nd:YAG laser operating at 1064 nm (infrared). The laser energy is attenuated to about 2–10 mJ per pulse by inserting circular apertures into the beam cavity. The ranges of instrument operating conditions are shown in Table 1. Under these conditions, crater size is $\leq$60 μm. Signal intensities were recorded for ^{26}Mg, ^{55}Mn, ^{43}Ca, ^{88}Sr, ^{138}Ba, and ^{208}Pb.

LA-ICP-MS analyses in the *M. edulis* shells were made in the middle of the calcite layer, from the umbo towards the edge, with a spacing of 150–250 μm (constant spacing within the same shell) between successive analysis sites. That way, successively deposited layers were sampled (Fig. 2a). For each series of 25 shell analyses, the mean signal intensity of the argon carrier gas was considered as the background. All signal intensities were background corrected before further treatment. ^{43}Ca was used as an internal standard for correcting instrument instability and drift. NIST 610 was used as an external standard for further correction of drift, for correction of day-to-day changes in instrument settings and for calibration. The signal intensities (average of 5 analyses) for the latter standard were determined for every series of 25 shell analyses. Accepted concentrations for NIST 610 were taken from Pearce et al. (1997). For a complete description of the evaluation of the LA-ICP-MS method for the analysis of Mg, Mn, Sr, Ba and Pb in *M. edulis* calcite, we refer to Vander Putten et al. (1999). In the latter study, we have shown that a precision better than 10% RSD can be obtained when using ^{43}Ca as an internal standard and NIST 610 as an external standard. This reproducibility is sufficient for analysis of the spatiotemporal variations of these elements in the shell. Since no sufficiently homogeneous matrix-matched reference material was (and is) available, accuracy could not be determined. Nevertheless, our results indicated that, at least for certain instrument settings, accuracy could be deteriorated as a result of the differences in ablation characteristics between samples and standard. When 2 overlapping analysis series were made in the calcite shell layer of *M. edulis* at different ICP-MS settings, a unidirectional, quite constant deviation of about 10% between corresponding data points was occasionally observed, i.e., the overlapping profiles were shifted with respect to each other by a constant factor. This implies that NIST 610 does not always sufficiently correct for day-to-day changes in instrument settings. In lack of a suitable matrix-matched standard, we decided to work with NIST 610 and to guarantee inter-comparability of our results by normalising all data with respect to one selected shell. The true analyte concentrations of this "reference" shell, and thus the accuracy of our results, are however unknown (Vander Putten et al., 1999).

Results are reported as the molar ratios of analyte to Ca. Electron microprobe analysis has shown that Ca is uniformly distributed over

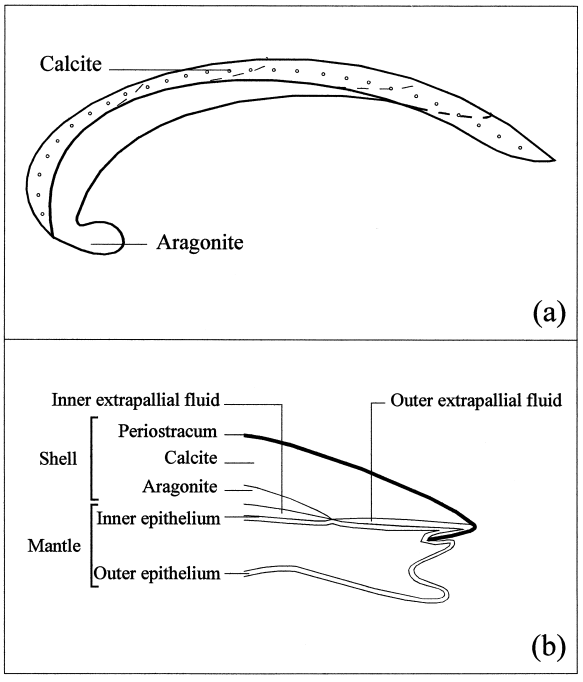

Fig. 2. Schematic view of *M. edulis*, sectioned along the axis of maximal growth, showing the mantle, the different calcium carbonate layers and the location of the LA-ICP-MS analysis sites within the calcite layer (dots). Dashed lines indicate the growth front of the calcite shell layer.

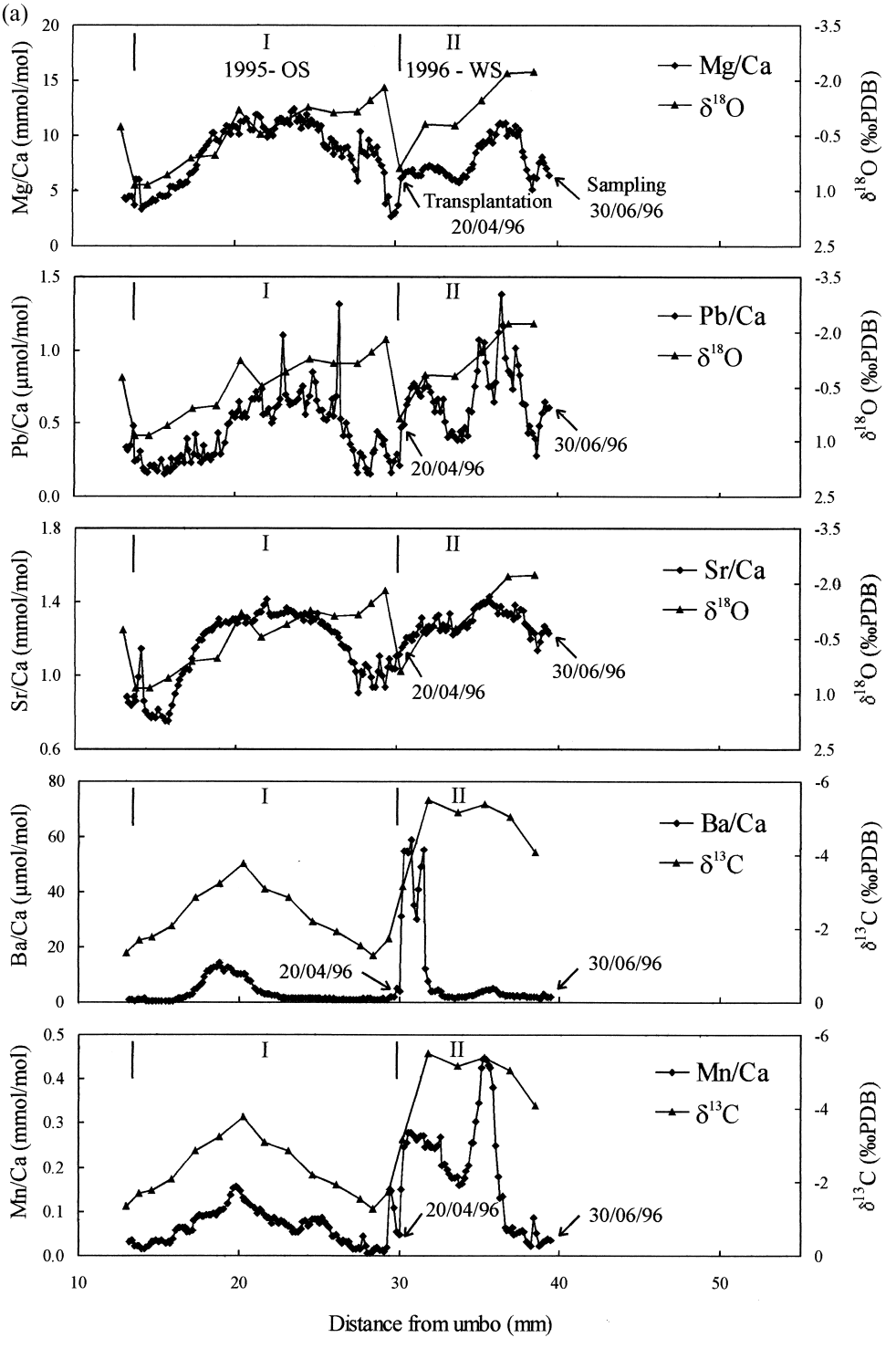

Fig. 3. a,b. Metal/Ca, $\delta^{13}C$ and $\delta^{18}O$ profiles in the calcite shell layer of two *M. edulis* specimens that grew initially in the OS and were transplanted on the 20th April 1996 to the WS where they were allowed to grow for a period of 10 weeks (a; shell 30) and 14 months (b; shell 50b) respectively. The moment of transplantation from the OS to the WS and the moment when the mussels were removed from the transplantation site are indicated on the metal/Ca profiles by an arrow, marked with the corresponding date. Note however that the arrow indicating the moment of collection does not necessarily coincide with the last data point as the shell may have stopped growing before the mussel was removed from the transplantation site. Two entire cycles (I, II) and the first part of a third one (III) have been delimited on the basis of the $\delta^{18}O$ maxima. Comparison with the position of the transplantation arrow shows that cycle I was formed in the OS whereas cycles II and III were formed in the WS.

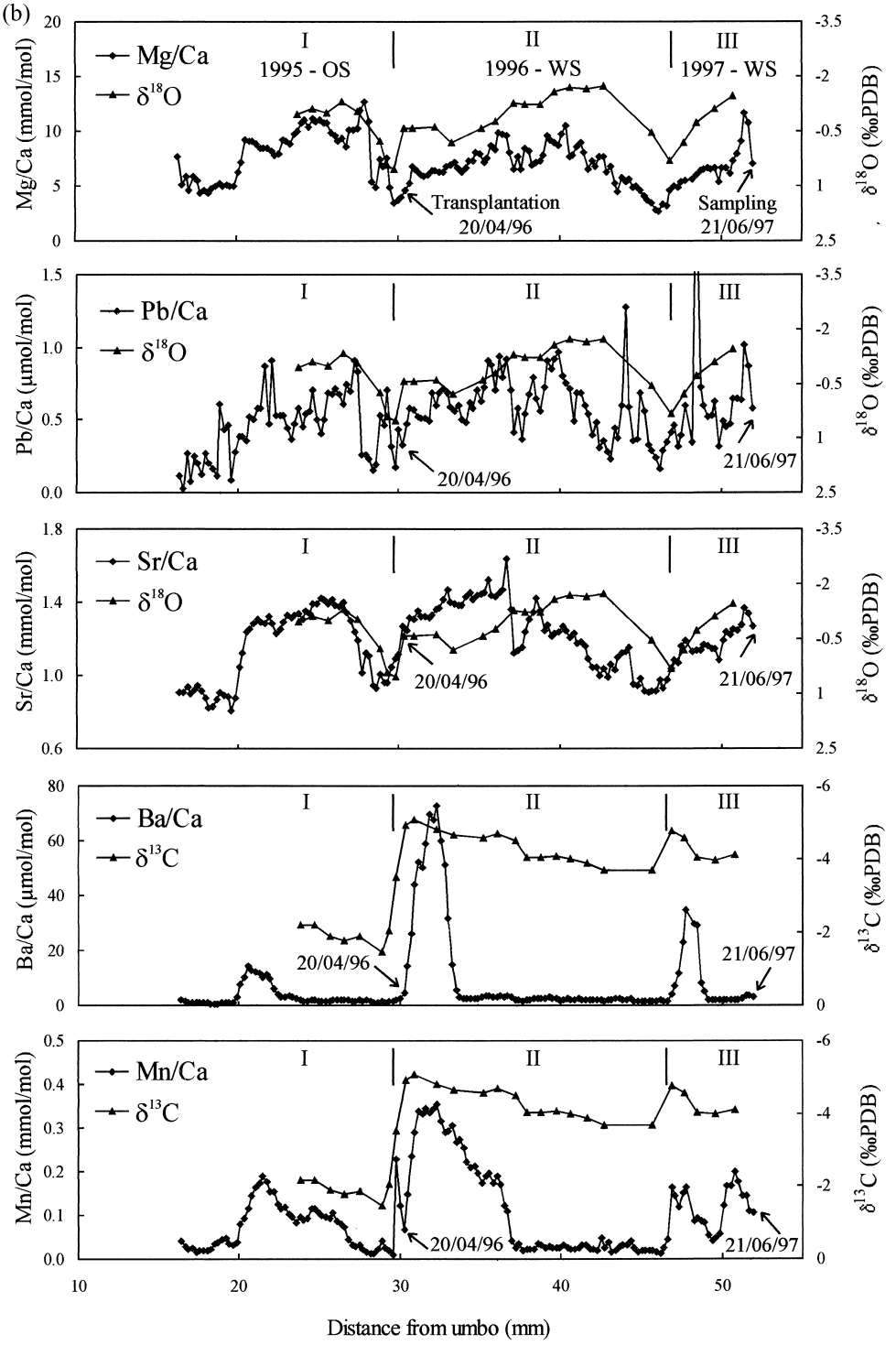

Fig. 3 (Continued)

the analysed *M. edulis* calcite sections, with a mean concentration of 398,000 ppm ± 5,600 SD (Vander Putten et al., 1999). A variation of 16,800 ppm (3 SD) on the mean Ca-concentration results in a variation of 4.2% on the analyte concentration, which is comparable to the precision of <10% RSD that can be obtained with LA-ICP-MS. Therefore, a constant Ca concentration was assumed over the analysed shell sections.

2.3.2. Determination of $\delta^{18}O$ and $\delta^{13}C$ profiles

For analysis of the skeletal $\delta^{18}O$ and $\delta^{13}C$ profiles, a shell section next to the one analysed by LA-ICP-MS was used. The shell surface was slightly polished in order to remove the periostracum. Subsequent samples of 1 to 3 mg were drilled from the calcite over the entire depth of the layer using a dental drill of 1 mm diameter. The sampling

direction was from the umbo towards the edge, with a spatial resolution of approximately 1 to 2 mm. Due to the lower spatial resolution, each of these samples corresponded to a number (5–10) of LA-ICP-MS sampling sites. A preliminary experiment was performed in order to verify if it was necessary to remove the organic shell matrix for isotopic analysis of the calcite. A thoroughly homogenised *M. edulis* calcite sample was split into 14 subsamples of ±2 mg. Half of the samples were analysed directly, while for the other half the organic shell matrix was removed by roasting the samples under vacuum at 380°C for 1 h prior to analysis (e.g., Klein et al., 1996b). The average $\delta^{18}O$ and $\delta^{13}C$ signals of the shell samples that were analysed directly were -1.02 ± 0.15 (1SD)‰ and -4.13 ± 0.08‰, respectively; the shell samples that were roasted before isotopic analysis had an average signature of -1.03 ± 0.09‰ and -4.13 ± 0.05‰ for $\delta^{18}O$ and $\delta^{13}C$ respectively. These results show that the organic shell matrix does not interfere significantly with the isotopic signal of the calcite. Therefore, it was decided to analyse the shell samples directly, without removing the organic material. The carbonate was transformed into CO_2 by reaction with anhydrous phosphoric acid at 25°C under vacuum. CO_2 was then extracted from the reaction mixture and trapped into a glass tube cooled with liquid N_2 after passing through successive liquid N_2 and cooled isopropanol freezing traps. The C and O isotopic composition of the CO_2 samples was determined with a dual inlet Finnigan Mat Delta E Isotope Ratio Mass Spectrometer. NBS 19 was used as a standard to report all isotopic signatures in ‰ relative to the V-PDB standard (Coplen, 1994). Precision, as determined by repeated analyses of a carrara working standard, was 0.1‰ for $\delta^{18}O$ and 0.01‰ for $\delta^{13}C$.

3. RESULTS

3.1. Seasonality of Shell Chemistry

Prior to transplantation, a few mussels from the batch originating from the Oosterschelde (OS) were kept apart for analysis. The skeletal Mn/Ca profiles of these mussels show a characteristic sharp peak at the posterior margin. This peak has been used as a marker for the onset of transplantation. The complete metal (Me)/Ca, $\delta^{18}O$ and $\delta^{13}C$ profiles of mussels 30 and 50b, which were collected 10 weeks respectively 14 months after transplantation to the Westerschelde (WS), are shown in Figure 3a,b (note that the first part of the stable isotope profiles of shell 50b is missing as the calcite layer in this zone was damaged and too thin to sample). All parameters exhibit cyclic variations with a similar periodicity. Two entire cycles (I, II) and the first part of a third one (III) have been delimited on the basis of the $\delta^{18}O$ maxima (note that there may be a slight misalignment—maximally 0.5 mm—between the stable isotope and LA-ICP-MS profiles as a result of the differences in sampling techniques and spatial resolutions). Comparison with the Mn/Ca peak marking the onset of transplantation shows that cycle I has been formed before transplantation while cycles II and III have been formed during the 14 months after transplantation. Note that the largest Me/Ca variations in cycle II are located in spring, during the first 10 weeks after transplantation. This is especially the case for Mn/Ca and Ba/Ca.

The skeletal $\delta^{18}O$ variations show that the periodicity in the Me/Ca- and stable isotope profiles is an annual one (Fig. 3a,b). Indeed, it is generally accepted that mollusc $\delta^{18}O$ is deposited in equilibrium with the surrounding water and hence is determined only by temperature and the oxygen isotopic composition of the water (e.g., Epstein, 1953). In the OS, where the mussels grew before transplantation, salinity is quite constant throughout the year: during 1995, salinity in Marollegat ranged between 28.4 and 30.2 (Hydrometeostation). Similarly, salinity in Hoofdplaat, a site 11 km downstream from the WS transplantation site, only ranged between 26.0 and 30.3 during the 14 months after transplantation (Hydrometeostation). Consequently, $\delta^{18}O$ of the seawater will have varied little during the life of the mussel, implying that the observed fluctuations in the shell $\delta^{18}O$ primarily reflect variations in water temperature. A decreasing skeletal $\delta^{18}O$ corresponds to an increasing temperature and vice versa. Cycles I and II in the $\delta^{18}O$ profiles thus reflect annual cycles of increasing temperature during spring and summer and decreasing temperature during fall and winter. In addition, the LA-ICP-MS profiles of shells collected on different moments have shown that cycle III was initiated between month 10 and 14 after transplantation (data not shown here). This observation confirms the annual periodicity of the cycles. Note that the increases in skeletal $\delta^{18}O$ are steeper than the decreases, indicating that shell growth was slower during fall–winter than during spring–(early) summer. The shell lengths of individuals sampled on different occasions during the transplantation experiment indicate that the shell growth rate was maximal during spring, more specifically during the first 10 weeks of the transplantation experiment. Indeed, at the end of June 1996, the shell length of 10 sampled individuals ranged between 37.5 and 43.5 mm, corresponding to an increase of about 8 to 14 mm in 10 weeks. The shell lengths of individuals sampled on subsequent occasions were as follows: 37.9–46.2 mm for 10 individuals sampled half of September (i.e., an increase of about 8 to 16 mm in 5 months), 39.7–50.8 mm for 10 individuals sampled at the end of November (i.e., an increase of about 10 to 21 mm in 7 months), and 40.3–50.3 mm for individuals sampled at the end of February the next year (i.e., an increase of about 10 to 20 mm in 10 months). Although actual shell growth rates were not measured, these data indicate that the rate at which new shell was added considerably slowed down after spring.

3.2. Temporal Variations of Mg, Sr and Pb

Within the same shell, there are similarities as well as differences between the profiles of the different elements. Roughly, Mg/Ca, Pb/Ca and Sr/Ca show a gradual variation, characterised by a broad maximum, over each annual cycle (Fig. 3a,b). The LA-ICP-MS profiles of shells collected at the end of summer show that in cycle II, this maximum is located in spring-early summer (data not shown here). This is corroborated by the $\delta^{18}O$ profile of shell 50b (Fig. 3b). A number of local variations are superimposed upon the general cyclic trend. This is most pronounced for the Pb/Ca profiles where some of the excursions are quite large and consist of only a few data points. As the Pb concentrations in the mussel shells lie close to the instrumental detection limit, some of these peaks may represent instrumental "noise". Nevertheless, it is clear that Mg/Ca, Sr/Ca and Pb/Ca roughly follow a similar trend. For cycle II, the three elements covary significantly in all of the analysed shells ($0.412 \leq r \leq 0.923$; $\alpha \leq 0.05$); for cycle I, the correlation coefficients are generally lower ($-0.162 \leq r \leq 0.879$). For the 10 analysed shells, Sr/Ca and Mg/Ca vary by a factor of 1.3 to 1.8 (with the exception of one outlier of 2.4) and 2.7 to 6.3 (with the exception of one outlier of 11.9) respectively over a given cycle; with the omission of high single point peaks, Pb/Ca varies by a factor of 3.1 to 11.0 over a given

cycle. There are no marked systematic differences between cycles I and II.

3.3. Temporal Variations of Ba, Mn and $\delta^{13}C$

The Ba/Ca variations in cycles I and II and the Mn/Ca variations in cycle II are dominated by a high peak in spring, followed by a broad minimum (Fig. 3a,b). In cycle I, the Mn/Ca peak extends over the entire cycle. The Ba/Ca peak is very narrow and is 4 to 7.3 times lower in cycle I than in cycle II (ratio between the peak maxima, for 10 individuals). In cycle II, the high Ba/Ca peak is systematically followed by a second peak which is 8.5 to 19.5 times lower than the first one (ratio between the peak maxima, for 10 individuals). In cycle I as well as cycle II, the Mn/Ca peak is broader than the Ba/Ca peak and has a roughly bimodal shape. As for Ba/Ca, the Mn/Ca peak in cycle I is 2 to 5 times lower than the one in cycle II (ratio between the peak maxima, for 10 individuals). In both cycles, the maximum of the high Ba/Ca peak approximately coincides with or slightly precedes the first local maximum of the bimodal Mn/Ca peak. The second smaller Ba/Ca peak in cycle II approximately coincides with the second local maximum of the bimodal Mn/Ca peak.

In cycle I of shell 30, $\delta^{13}C$ covaries quite well with Mn/Ca (Fig. 3a). In particular, the $\delta^{13}C$ minimum coincides with the Mn/Ca maximum. In cycle II, $\delta^{13}C$ exhibits a minimum during the period of high Mn/Ca and, at least for shell 30, the local $\delta^{13}C$ minima coincide with the local maxima of the bimodal Mn/Ca peak (Fig. 3a,b).

3.4. Reproducibility of Shell Composition Between Individuals

Figure 4 shows the Me/Ca distribution in shell formed after transplantation for four mussels (29, 30, 32 and 34) sampled 10 weeks after transplantation to the WS. The increase in shell length over the considered period (72 days) varied from 9.5 mm for mussel 30 to 13.5 mm for mussel 34. The profiles of the different shells were matched by assigning a date to each measured value. For this purpose, it was assumed that the individual shell growth rate remained constant over the entire period after transplantation. For mussel 30, the $\delta^{18}O$ profile for shell formed after transplantation covaries with the measured temperature profile (Fig. 5a). This suggests that this shell did indeed grow quite uniformly after transplantation, at least on the timescale of the $\delta^{18}O$ analysis (i.e., about 8 to 15 days). Nevertheless, it should be stressed that the shell growth rate was not necessarily constant on a daily timescale. Moreover, for mussels 29, 32 and 34, the assumption of uniform shell growth remains purely hypothetical. Figure 4 shows that the general Me/Ca trends, in shape as well as in amplitude, are similar for all individuals. A striking feature is the reproducible location of the Ba/Ca and Mn/Ca peaks. Note however that the shapes of these peaks in shell 30 deviate from the general trend. For Sr/Ca and Pb/Ca, and to a lesser extent also for Mg/Ca, it is shell 32 that deviates from the general trend.

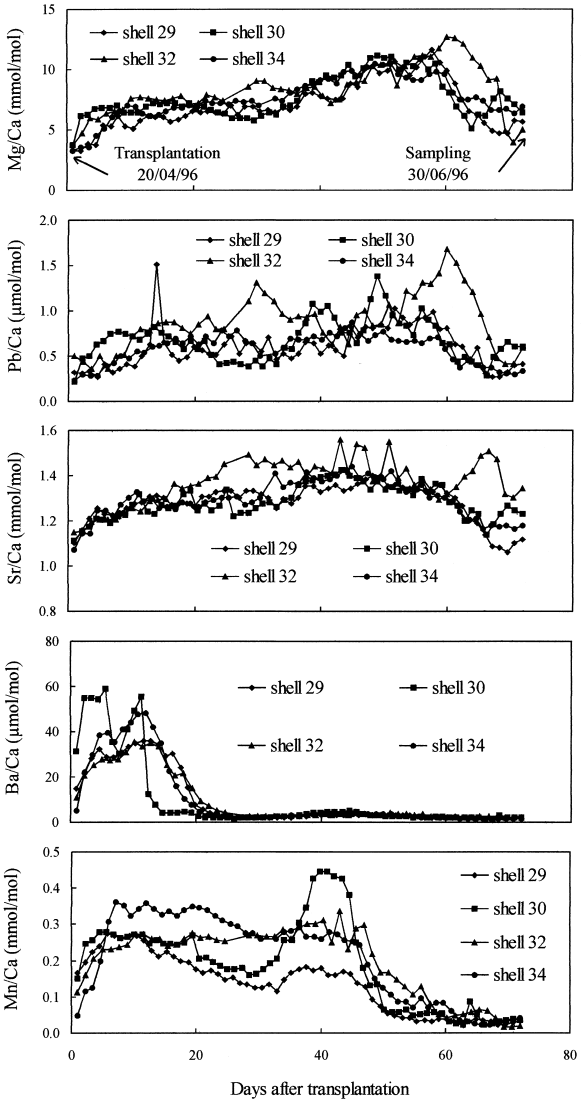

Fig. 4. Metal/Ca profiles in the calcite shell layer of four *M. edulis* specimens that grew in the WS from the 20th April 1996 until the 30th June 1996; the data points correspond to shell deposited during this period. Arrows indicate the moment of transplantation from the OS to the WS and the moment when the mussels were removed from the transplantation site. The profiles are shown as a function of time whereby dates were assigned to each measured value by assuming a constant shell growth rate over the period of interest. The increase in shell length over this period (72 d) varied from 9.5 mm for mussel 30 to 13.5 mm for mussel 34.

4. DISCUSSION

Although mollusc shell chemistry is undoubtedly influenced by the physicochemical properties of the ambient seawater, it is becoming increasingly clear that relationships between metal (Me)/Ca and $^{13}C/^{12}C$ ratios in shells and those in water are complicated by physiological controls. In molluscs, calcification occurs within the extrapallial fluid (EPF), which is secreted by the mantle and is isolated from the external medium (Wilbur and Saleuddin, 1983; Fig. 2b). The composition of the EPF might be significantly altered with respect to seawater due for instance to the influence of mantle metabolic activity on the transport of metals through the mantle (e.g., Klein et al., 1996b), to the contribution of metals and carbon from metabolic sources (e.g., Tanaka et al., 1986; Klein et al., 1996b) or

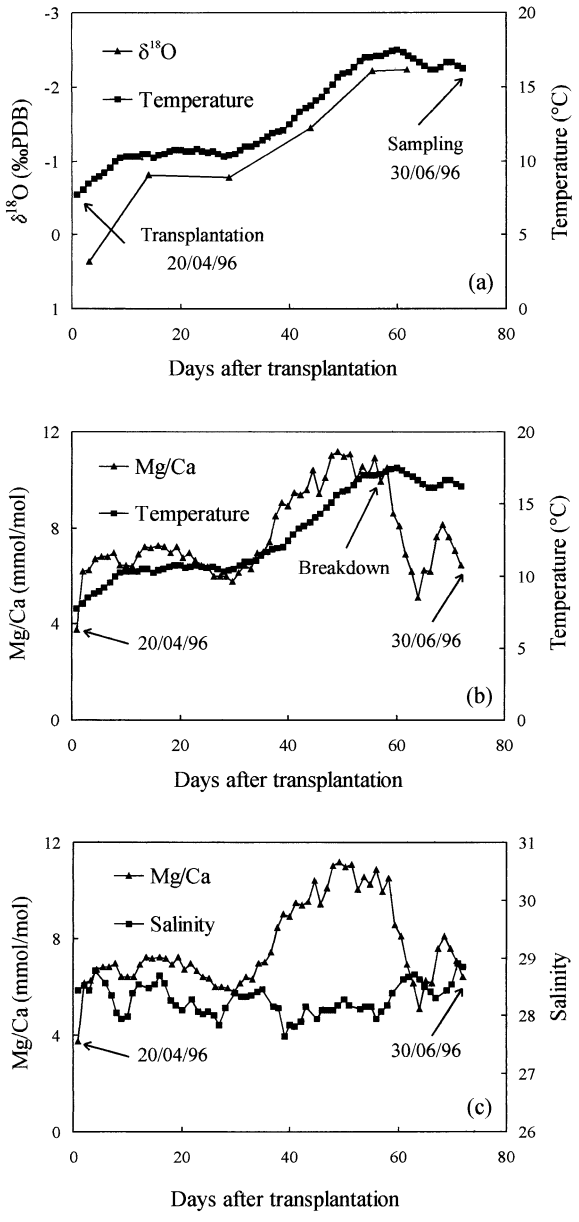

Fig. 5. a,b,c. $\delta^{18}O$ profile (a) and Mg/Ca profile (b,c) in the calcite shell layer of a *M. edulis* specimen (shell 30) that grew in the WS from the 20th April 1996 until the 30th June 1996; the data points correspond to shell formed during this period. Arrows indicate the moment of transplantation from the OS to the WS and the moment when the mussel was removed from the transplantation site. Dates were assigned to the shell profiles by assuming a constant shell growth rate over the period of interest. The profiles are shown together with temperature (a,b) and salinity (c) measured at Hoofdplaat, a location 11 km downstream from the site where the mussels grew.

to organic complexation (Crenshaw, 1972). In addition, metals are not necessarily incorporated into the calcite crystal structure but can also be adsorbed onto the skeletal organic matrix (e.g., Lingard et al., 1992) or entrapped as separate mineral phases (e.g., Fritz et al., 1990) Furthermore, the skeletal trace element and carbon isotope composition may be (in part) kinetically controlled (e.g., Stecher et al., 1996).

4.1. Magnesium, Strontium and Lead

4.1.1. Magnesium

The skeletal Mg/Ca variations observed in the present study (Mg/Ca varies by a factor of 3 to 6 over a given cycle, see earlier, 3.2.) cannot be explained solely on the basis of seasonal variations in the seawater Mg/Ca ratio. Dodd and Crisp (1982) showed that the Mg/Ca ratios of most estuarine waters only differ significantly from the open ocean ratios at salinities below 10. As the annual salinity fluctuations in the successive environments of growth in the present study are quite small (see earlier, 3.1.), it is clear that the seasonal variations in the shell Mg/Ca ratio must be caused by processes other than changes in the seawater Mg/Ca ratio.

Several authors have reported on a relationship between Mg/Ca in mollusc shell calcite and temperature. Dodd (1965) has observed a seasonal variation, correlated with temperature, in the Mg content of *M. edulis* shells. In a more recent study, Klein et al. (1996a) demonstrated that Mg/Ca variations in the shell of *M. trossulus* (formerly *M. edulis*) show an excellent covariation with sea-surface temperature. This covariation is described by the following equation: (Mg/Ca * 1000) = 0.30 ($\pm$0.04) * T + 2.25 ($\pm$0.63) (r^2 = 0.74). In the present study, Mg/Ca in shells 29, 30, 32 and 34 covaries significantly with water temperature during the 10 weeks following transplantation ($0.58 < r < 0.65$ for the individual shells; $\alpha \leq 0.01$), at least if we assume a constant shell growth rate over the considered period (see earlier, 3.4.). The overall covariation is described by the following equation: (Mg/Ca * 1000) = 0.39 ($\pm$0.03) * T + 2.61 ($\pm$0.44) (r = 0.61). However, when examining the element profiles in detail, it becomes clear that for each of the four shells a period of close covariation between Mg/Ca and temperature ($0.90 < r < 0.96$ over the first 50 to 63 days after transplantation) is followed by an abrupt breakdown in this covariation (e.g., Fig. 5b for shell 30). The moment at which the breakdown occurs, i.e., 50 to 63 days after transplantation, as well as the parameters of the linear regression before the breakdown are similar for all four of the shells (Fig. 6). The overall Mg/Ca temperature relationship before the breakdown is described by the following equation: (Mg/Ca * 1000) = 0.70 ($\pm$0.02) * T $-$ 0.63 ($\pm$0.29) (r = 0.91). As the breakdown in the shell Mg/Ca temperature covariation does not coincide with a marked salinity change (Fig. 5c), the sudden decrease in skeletal Mg/Ca is not likely to be caused by a change in the seawater Mg/Ca ratio or in the absolute Mg concentration. It should be stressed that there is an uncertainty on the skeletal timescales (see earlier, 3.4.) and thus also on the reported correlation coefficients. Nevertheless, it is clear that there can be no constant Mg/Ca temperature relationship over the considered period.

For mussels that have remained in the WS for 5, 7, 10 and 14 months, no unambiguous skeletal timescale can be established since the actual variations in shell growth rate over the considered period are unknown. Consequently, a direct comparison with the water temperature profile is difficult. Nevertheless, in a first approach, a timescale has been constructed in the following way. First, we made the assumption that the two successive skeletal Ba/Ca peaks formed after transplantation were deposited synchronously for all individuals, more specifically

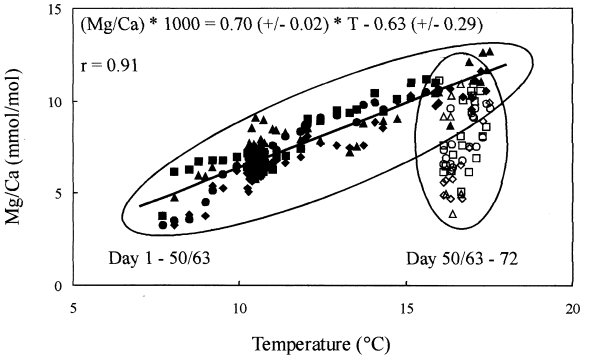

Fig. 6. Mg/Ca variations in the calcite shell layer of four *M. edulis* specimens (shells 29, 30, 32 and 34; see symbols in Fig. 4), shown as a function of water temperature. The mussels grew in the WS from the 20th April 1996 until the 30th June 1996; the data points correspond to shell formed during this period. Filled dots correspond to the period where there is a close covariation between skeletal Mg/Ca and temperature, i.e., the first 50–63 d after transplantation; open dots correspond to the period after the abrupt breakdown in this Mg/Ca temperature covariation (e.g., Fig. 5b for shell 30). The regression equation is based on the data points represented as filled dots.

during the first 10 weeks after transplantation and that, in analogy with shell 30 (see earlier, 3.4.), the shell growth rate over this period was constant. Furthermore, we assumed that after this period shell material was still formed at a constant but different rate until the moment when the mussels were removed from the transplantation site. During the (inferred) initial 10 weeks following transplantation, a period where skeletal Mg/Ca and temperature covary relatively well is again followed by a breakdown in this covariation (e.g., Fig. 7a for shell 161). The Mg/Ca temperature covariation is sometimes slightly different and less pronounced than for shells 29, 30, 32 and 34, but this could be caused in part by the error that is made in assigning the timescales. After the breakdown, the original Mg/Ca temperature relationship is not recovered for any of the shells. More specifically, the Mg/Ca ratios after the breakdown are always lower with respect to temperature than values expected from the initial Mg/Ca temperature relationship (e.g., Fig. 7a). Even though the actual shell growth rates are unknown and large errors may be made in the assignment of the timescales, the latter observation remains valid. For at least one individual, Mg/Ca appears to follow temperature again after the breakdown of the initial Mg/Ca temperature covariation, albeit with a different Mg/Ca temperature proportionality than before (Fig. 7a). However, since the actual shell growth rate is unknown, the latter observation remains speculative. The $\delta^{18}O$ profiles for shell formed before transplantation confirm the absence of a constant Mg/Ca temperature relationship over the year. For shell 30, Mg/Ca in cycle I initially increases with increasing temperature (reflected by decreasing $\delta^{18}O$) but at a certain moment, Mg/Ca decreases while temperature continues to increase (Fig. 3a).

Our observations do not preclude that temperature may have an effect on skeletal Mg incorporation, either directly or through a physiological factor that covaries with temperature. However, as there is clearly no constant Mg/Ca temperature relationship within the same shell, temperature is certainly not the only controlling factor. Perhaps, an (in)direct temperature

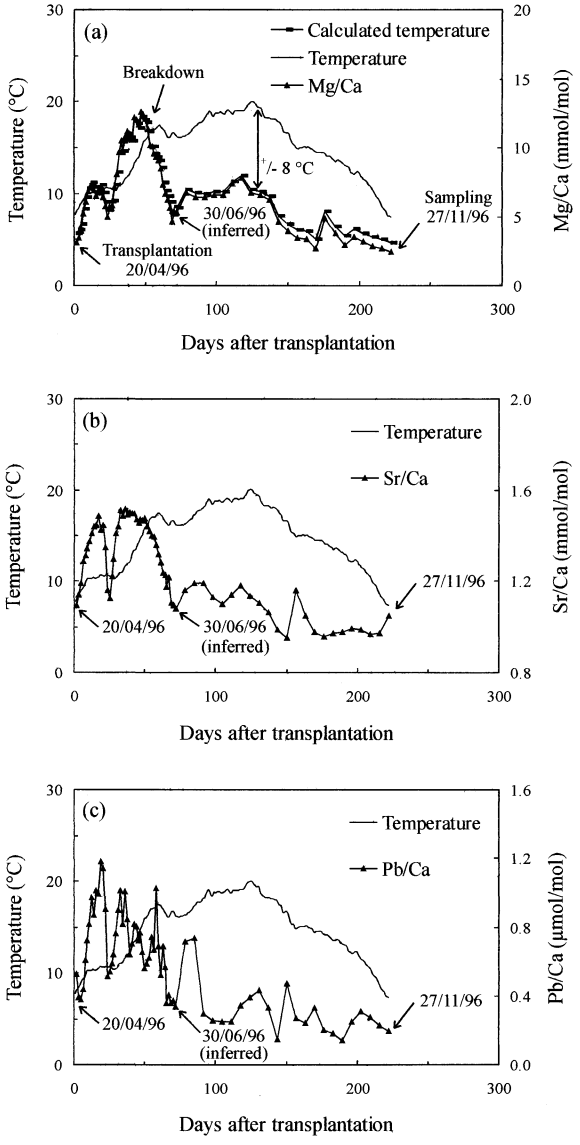

Fig. 7. a,b,c. Profiles of Mg/Ca (a), Sr/Ca (b) and Pb/Ca (c) in the calcite shell layer of a *M. edulis* specimen (shell 161) that grew in the WS from the 20th April 1996 until the 27th November 1996; the data points correspond to shell formed during this period. Arrows indicate the moment of transplantation from the OS to the WS and the moment when the mussel was removed from the transplantation site. The shell profiles are shown as a function of time together with the corresponding measured water temperature profile. Dates were assigned to the shell profiles by assuming a constant shell growth rate between the 20th April 1996 and the 30th June 1996 and a different, but also constant shell growth rate between the 30th June 1996 and the moment when the mussel was sampled. The end of the second Ba peak was taken as the point on the shell corresponding to the 30th June 1996. Also shown in (a) is the theoretical temperature profile, calculated on the basis of the skeletal Mg/Ca profile and the Mg/Ca temperature relationship that was established for shells 29, 30, 32 and 34 (Fig. 6).

control on skeletal Mg incorporation is combined with a seasonal physiological effect, with the latter triggering the observed breakdown in the Mg/Ca temperature covariation. At the moment, one can only speculate on the nature of the (additional) controlling factors. Hartley and Mucci (1996) suggested that

variations in the microtopograhic properties of naturally occurring calcites, possibly as a result of adsorbed organic matter (Morse and Mucci, 1984), might explain some of the variability in the Mg content of modern marine calcite cements. This speculation was based on the observation that simultaneously deposited nonequivalent faces of one and the same calcite crystal may contain different concentrations of Mg, Sr, Fe and Mn (e.g., Reeder and Paquette, 1989). This pattern, referred to as sector zoning, results from differences in the solution–crystal partitioning of trace elements between nonequivalent crystal faces, presumably as a result of differences in surface structure. Moreover, Reeder and Grams (1987) and Reeder and Prosky (1986) found that when sector zoning is observed, all trace elements (i.e., Mg, Mn, Fe and Sr) are preferentially enriched in the same sector. Applied to our study, seasonal variations in the calcite crystal properties, possibly as a result of changes in the abundance or composition of the organic matrix, might have an effect on the skeletal incorporation of Mg, Mn, Sr and possibly also Pb. Alternately, metals might be directly adsorbed on the organic shell matrix. Changes in the content or the nature of this matrix might then lead directly to variations in the skeletal metal incorporation. The rough covariation that has been observed between shell calcite Mg/Ca and S/Ca (the latter assumed to reflect the content of organic matrix), both within and between shells of *M. edulis* (Lorens and Bender, 1980; Rosenberg and Hughes, 1991), might indeed be indicative of the participation of the organic matrix in Mg incorporation. However, microprobe analysis has shown that the Ca concentration in a *M. edulis* calcite section, similar to the ones analysed in the present study, does not show a seasonal variation (Vander Putten et al., 1999). Consequently, it seems unlikely that the amount of organic matter is highly fluctuating over the analysed calcite sections. Nevertheless, a seasonal variation in the nature or micro-distribution of the organic matrix can not be excluded. A study of the micro-structural properties of *M. edulis* calcite might provide more insight into the mechanism(s) governing trace metal incorporation.

Regardless of which factors are controlling the incorporation of Mg into the shell, our results clearly show that Mg/Ca in *M. edulis* calcite cannot be used directly as a high resolution temperature proxy. Indeed, the error that is made when disregarding the fact that the Mg/Ca temperature relationship may vary over the year can be quite large. For instance, Figure 7a shows the temperature profile inferred from the Mg/Ca profile of shell 161. This temperature profile was calculated on the basis of the Mg/Ca temperature relationship established for shells 29 to 34 (see earlier). The average discrepancy between the calculated and actual temperature after the breakdown in the Mg/Ca temperature "covariation" amounts to 8°C.

4.1.2. Strontium

Lorens and Bender (1980) found that the Sr/Ca ratio in the calcite shell layer of mussels grown under controlled laboratory conditions increased linearly with solution Sr/Ca. However, the skeletal Sr/Ca variations observed in the present study (Sr/Ca varies by a factor of 1.3 to 1.8 over any given cycle, see earlier, 3.2.) are too large to be explained solely on the basis of variations in the seawater Sr/Ca ratio. Indeed, Dodd and Crisp (1982) showed that the Sr/Ca ratios of most estuarine waters only differ significantly from the open ocean ratios at salinities below 10. In view of the quite small annual salinity variations in the OS as well as at the WS transplantation site (see earlier, 3.1.), it thus seems unlikely that variations in the seawater Sr/Ca ratio were large enough to give rise to the seasonal variations in skeletal Sr/Ca.

Dodd (1965) has reported a seasonal variation, correlated with temperature, in the Sr content of *M. edulis* shells. However, whereas skeletal Mg/Ca in the present study to some extent covaries with temperature, at least during some periods of the year (e.g., Fig. 5b, Fig. 7a), this is not the case for Sr/Ca (Fig. 7b). Apparently, neither temperature variations, nor changes in solution chemistry can entirely explain the observed skeletal Sr/Ca variations. If the former processes do have an effect on the incorporation of Sr into the shell, there should at least one or more additional controlling factors. Klein et al. (1996b) suggested that the relationship between Sr/Ca ratios in seawater and the ones in the calcite shell layer of *M. trossulus* is complicated by the influence of mantle metabolic activity. Briefly, these authors suggested that the skeletal Sr/Ca ratio of individuals with a negligible mantle metabolic activity closely follows the seawater Sr/Ca ratio, whereas the skeletal Sr/Ca ratio in animals with a higher mantle metabolic activity is modified by the rate of Ca-pumping across the mantle. It is assumed that the Ca concentration in the EPF of the latter mussels is maintained at approximately constant levels while the Sr concentration covaries with seawater Sr. As Sr behaves conservatively during estuarine mixing, skeletal Sr/Ca variations in mussels with a high mantle metabolic activity may register variations in salinity (Klein et al., 1996b). Although the mussels in the present study presumably have a high metabolic activity (see below, discussion on $\delta^{13}C$), skeletal Sr/Ca does not show a positive covariation with salinity. On the contrary, if we assume a constant shell growth rate over the first 10 weeks after transplantation, skeletal Sr/Ca and salinity appear to exhibit an opposite trend ($-0.36 \leq r \leq -0.54$ for shells 29, 30, 32 and 34). Nevertheless, this does not preclude that metabolic activity may, in some way, play a role in regulating the incorporation of Sr in the studied shells.

Whereas experimental studies have shown that the incorporation of Sr into nonskeletal calcite overgrowths increases with increasing precipitation rate (e.g., Lorens, 1981), there are as yet no indications that the incorporation of Sr into mollusc shell calcite is kinetically controlled. Neither Sr/Ca variations within the calcite shell layer of *M. trossulus* (Klein et al., 1996b) nor inter-specimen differences in the skeletal Sr content of *M. edulis* (Lorens and Bender, 1980) were correlated with variations in shell growth rate. Nevertheless, our data do not preclude the existence of a kinetic effect. Several observations indicate that shell growth considerably slowed down after the initial 10 weeks after transplantation. A first indication comes from shell length measurements (Results, 3.1). Second, if a skeletal timescale is constructed as described earlier (see discussion on Mg), the inferred shell growth rate decreases by a factor of about three after the first 10 weeks following transplantation. For instance, for shell 161 (Fig. 7a,c), the shell growth rate decreases from 0.15 $mm \cdot day^{-1}$ during the initial 10 weeks to 0.04 $mm \cdot day^{-1}$ thereafter. These seasonal variations in growth rate appear to be reflected in the shell Sr/Ca profiles in that the average Sr/Ca ratio for the first 10 weeks

after transplantation (zone associated with the occurrence of two successive Ba/Ca peaks; see earlier) is higher than for the following period (e.g., Fig. 3b, Fig. 7b). However, further experimental work is required to confirm this hypothesis and to verify whether smaller scale Sr/Ca variations could be associated with short term changes in shell growth rate. As has been suggested earlier for Mg/Ca, Sr/Ca variations might also be caused by seasonal variations in the nature or micro-distribution of the organic matrix. The latter process might lead to variations in the amount of adsorbed cations or to changes in the surface structure of the calcite crystals, leading in turn to variations in the solution–crystal partitioning of the cations. Furthermore, the incorporation of Sr into the shell might be directly influenced by the skeletal Mg content. Mucci and Morse (1983) reported on a covariation between the Mg content and the Sr partitioning coefficient for experimentally precipitated calcite overgrowths. Similarly, Carpenter and Lohmann (1992) observed a covariation between Sr and Mg in Holocene abiotic calcite and in biotic calcite (on the taxonomic level). Mucci and Morse (1983) proposed the following mechanism: since Mg^{2+} has a smaller ionic radius than Ca^{2+}, the incorporation of the former cation causes a lattice distortion (Goldsmith et al., 1961) so that a site is created where a cation larger than Ca^{2+}, such as Sr^{2+}, could be more easily accommodated. Note that this might also apply for Pb.

4.1.3. Lead

Skeletal Pb presumably originates from both dissolved and particulate Pb. While Pitts and Wallace (1994) showed that the Pb content of aragonitic *Mya arenaria* shells was related to dissolved Pb concentrations, Bourgoin (1990) found a significant correlation between Pb in the aragonitic layer of *M. edulis* shells and suspended particulate Pb concentrations. However, the skeletal Pb/Ca variations observed in the present study may not be related to seasonal variations in aquatic Pb concentrations. Although the skeletal Pb/Ca profiles show several pronounced excursions (which might represent instrumental noise or highly localised inclusions), there is an underlying seasonal trend with a broad maximum during spring and early summer (e.g., Fig. 3b). By contrast, suspended particulate Pb concentrations near the WS transplantation site were about 2 times lower at the end of May 1996 (33.4 $\mu g \cdot g^{-1}$) than in February (63.2 $\mu g \cdot g^{-1}$), October (66.1 $\mu g \cdot g^{-1}$) and December (76.2 $\mu g \cdot g^{-1}$) of the same year; dissolved Pb concentrations in May 1996 (0.081 $\mu g \cdot l^{-1}$) were similar to those in October (0.088 $\mu g \cdot l^{-1}$) but 1.5 to 2 times lower than in February (0.16 $\mu g \cdot l^{-1}$) and December (0.11 $\mu g \cdot l^{-1}$) (Koen Parmentier, personal communication). This corroborates earlier results of Valenta et al. (1986) and Baeyens et al. (1998a), indicating that dissolved Pb concentrations in the WS were lower in summer than in winter. However, direct comparison with the high resolution skeletal Pb/Ca profiles requires aquatic Pb data at a much higher temporal resolution. Moreover, total dissolved and particulate Pb concentrations are not necessarily representative for the bioavailable concentrations. Nevertheless, our preliminary findings indicate that seasonal Pb/Ca variations in the shell may be related to processes other than variations in aquatic Pb concentrations. This needs to be taken into account when attempting to use *M. edulis* shell chemistry for the high resolution monitoring of Pb pollution.

The observed similarity of the Mg/Ca and Pb/Ca profiles (see earlier, 3.2) and the covariation between Mg/Ca and temperature (albeit poor and not persistent over the year; e.g., Fig. 5b, 6 and 7a), lead us to verify if there is any relationship between skeletal Pb/Ca and temperature. However, the shape of the temperature profile is clearly not reflected in the skeletal Pb/Ca profile (e.g., Fig. 7c). Apparently, temperature variations are of minor (or of no) importance in controlling the incorporation of Pb into *M. edulis* shell calcite. There is as yet insufficient information to determine what might be the main processes governing the observed skeletal Pb/Ca trends. Perhaps, Pb/Ca variations are caused by seasonal variations in the nature or the micro-distribution of the organic matrix (see discussion on Mg and Sr). Alternately, as been suggested earlier for Sr, the partitioning of Pb between the EPF and the shell might be dependent on the Mg content of the shell.

4.2. Barium, Manganese and $\delta^{13}C$

4.2.1. Barium

The annual skeletal Ba/Ca cycles are dominated by one high, narrow peak, which is systematically located in spring (e.g., Fig. 3a,b) and is quite reproducible between individuals (Fig. 4). Similar sharp Ba/Ca increases, at various times during the year, were observed in the aragonitic shells of *Mercenaria mercenaria* and *Spisula solidissima* (Stecher et al., 1996). Stecher et al. suggested that these peaks might be the result of high levels of particulate Ba, associated with diatom blooms. Elevated levels of Ba, both as suspended particulate Ba and sedimentary barite, have been shown to be linked with oceanic regions of high primary productivity (Goldberg and Arrhenius, 1958; Chow and Goldberg, 1960; Dehairs et al., 1980; Dehairs et al, 1987; Bishop, 1988). It has been suggested that this phenomenon results from the precipitation of barite inside organic-rich, siliceous microenvironments, formed primarily by assemblages of decaying diatoms (Bishop, 1988; Stroobants et al., 1991). As *M. mercenaria* and *S. solidissima* are filter-feeding bivalves, the Ba-rich particles are supposedly ingested as food. Once inside the digestive tract, Ba may be metabolised, at least in part, by being shunted to the EPF and sequestered into the shell (Stecher et al., 1996). Since *M. edulis* is also a filter-feeder, similar processes might be responsible for the skeletal Ba/Ca increases in spring that were observed in the present study. Our results indeed corroborate the suggestions of Stecher et al. (1996) on a relationship between skeletal Ba/Ca and primary production. If we assume a constant shell growth rate over the first 10 weeks after transplantation (see earlier, 3.4.), the locations (but not the magnitudes) of the 2 successive Ba/Ca peaks in cycle II coincide approximately with the highest chlorophyll *a* peaks observed in 1996 (e.g., Fig. 8a for shell 30; data for Vlissingen, a site located 18 km from the WS transplantation site; MWTL programs, RIKZ). Furthermore, the $\delta^{18}O$ profile for shell 30 indicates that the Ba/Ca peak in shell deposited before transplantation was formed in spring (Fig. 3a, cycle I). Hence, this peak might coincide with the 1995 chlorophyll *a* maximum in the OS (Yerseke) which was located at the end of May (MWTL programs, RIKZ). The

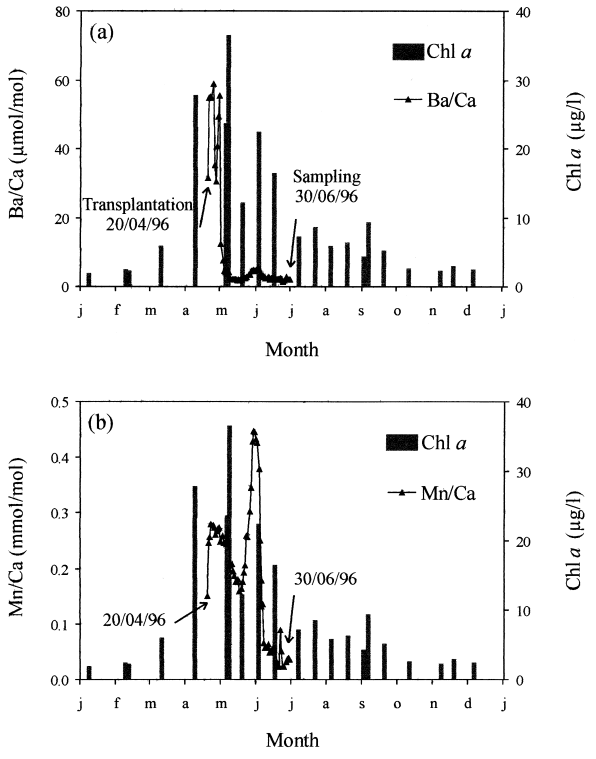

Fig. 8. a,b. (a) Ba/Ca and (b) Mn/Ca profiles in the calcite shell layer of a *M. edulis* specimen (shell 30) that grew in the WS from the 20th April 1996 until the 30th June 1996; the data points correspond to shell formed during this period. Arrows indicate the moment of transplantation from the OS to the WS and the moment when the mussel was removed from the transplantation site. Dates were assigned to the shell profiles by assuming a constant shell growth rate over the period of interest. Bars represent chlorophyll *a* concentrations measured at Vlissingen, a site located approximately 18 km downstream from the site where the mussel grew.

Ba/Ca peak in cycle I was on average 5.2 ± 1.2 SD times lower than the one in cycle II (for the analysed 10 individuals). This might result directly from differences in algal biomass as the 1995 chlorophyll *a* maximum in Yerseke was about 3 times lower than the 1996 maximum in Vlissingen (MWTL programs, RIKZ). Other possible explanations are differences in (bioavailable) Ba concentrations associated with the respective blooms or ontogenetic variations in the uptake and incorporation of Ba into the shell.

Our observations thus indicate that the sharp Ba/Ca peaks provide excellent markers for the spring phytoplankton blooms. Nevertheless, it is obvious that there is no linear relationship between skeletal Ba/Ca and chlorophyll *a*. Indeed, the Ba/Ca-chlorophyll *a* ratio for the first peak in cycle II is about 7 times larger than for the second one (Fig. 8a; Ba/Ca-chlorophyll *a* ratio of 1.4 ± 0.3 SD for the first peak versus 0.19 ± 0.03 SD for the second one, for 10 individuals). This apparent discrepancy might be caused by physiological effects or by variations in the (bioavailable) Ba concentrations associated with the successive blooms, possibly as a result of a difference in algal species. Further studies on the relationship between Ba and primary production and on the effect of physiological variables on skeletal Ba incorporation will be required to verify if skeletal Ba can be used as a quantitative primary productivity proxy.

4.2.2.Manganese

As far as we know, no one has yet related the distribution of Mn in mollusc shells to environmental or biological variables. In the present study, the Mn/Ca cycle in shell formed after transplantation (cycle II) is dominated by a high peak in spring (e.g., Fig. 3a,b, Fig. 4). The Mn/Ca profiles of shells 29, 30, 32 and 34 show that the location of this peak coincides with the period of the year when chlorophyll *a* concentrations were maximal (e.g., Fig. 8b for shell 30; MWTL programs, RIKZ). If we assume a constant shell growth rate over the period of interest, the positions (although not the magnitudes) of the twin Mn «peaks» correspond to successive chlorophyll *a* peaks. In addition, the $\delta^{18}O$ profile for shell 30 indicates that the Mn/Ca maximum in shell deposited before transplantation is located in spring (Fig. 3a, cycle I) and might thus coincide with the 1995 chlorophyll *a* maximum in the OS (Yerseke) at the end of May (MWTL programs, RIKZ). The second local Mn/Ca maximum in cycle I might correspond to the second local chlorophyll *a* maximum at the end of July the same year. These findings are indicative of a relationship between primary production and increased incorporation of Mn into the shell. This hypothesis seems plausible as natural phytoplankton blooms have been shown to be associated with an increase in suspended particulate Mn (Morris, 1971; Sunda and Huntsman, 1988). This can be the result of several processes. First, algae efficiently take up and accumulate Mn (II) intracellularly (Sunda and Huntsman, 1985). Furthermore, certain types of phytoplankton may catalyse the oxidation of Mn. In colonies of *Phaeocystis*, in dense algal populations and at the surface of large phytoplankton cells, photosynthesis generates high pH (>9) microenvironments where insoluble Mn oxides are formed (Richardson et al., 1988; Lubbers et al., 1990; Richardson and Stolzenbach, 1995). It is well known that the spring bloom in the North Sea is characterised by a *Phaeocystis* predominance, either in its colonial or its single-cell stage (Lancelot, 1984). Consequently, as for Ba/Ca, increases in the skeletal Mn/Ca ratio might reflect elevated particulate Mn concentrations associated with the (spring) phytoplankton bloom. The fact that the Mn/Ca peak in shell deposited before transplantation is on average 3.3 ± 1.1 SD times lower than the peak formed after transplantation (ratio between peak maxima, for 10 individuals) might then result directly from differences in algal biomass (see chlorophyll *a* data in discussion on Ba). Other possible explanations are differences in (bioavailable) Mn concentrations associated with the respective blooms or ontogenetic variations in the uptake and incorporation of Mn into the shell.

The episodic increases in skeletal Mn and Ba thus appear to be governed by similar processes, i.e., an increase in (available) particulate concentrations associated with the phytoplankton bloom. However, although the (local) Mn/Ca maxima coincide with the (local) Ba/Ca maxima, the Mn/Ba ratio varies over the year. We propose that the skeletal Ba/Ca and Mn/Ca increases may each be associated with the occurrence of specific types of phytoplankton.

4.2.3. $\delta^{13}C$

Seawater Dissolved Inorganic Carbon (DIC) can be expected to be a major source for skeletal carbon. However, the skeletal $\delta^{13}C$ variations observed in the present study (Fig. 3a,b) appear to be opposite to the seasonal $\delta^{13}C_{DIC}$ trend. Several authors have reported on a relationship between $\delta^{13}C_{DIC}$ and primary production. Mook (1970) and Mook and Tan (1991) reported that, whereas marine $\delta^{13}C_{DIC}$ shows little variation over the year, small seasonal variations may result from the preferential uptake of isotopically light CO_2 during primary production. More recently, Hellings et al. (1999a,b) showed that $\delta^{13}C_{DIC}$ in the freshwater and brackish part of the Schelde estuary is low in winter and increases in spring and summer because of the preferential uptake of ^{12}C by phytoplankton during the bloom. Although $\delta^{13}C_{DIC}$ variations at our study sites (WS transplantation site and OS) were not measured, we assume that the intense primary production in spring (inferred from the chlorophyll *a* data, see discussion on Ba) will lead to an increase in $\delta^{13}C_{DIC}$ during this period. By contrast, the skeletal $\delta^{13}C$ cycles are characterised by a minimum in spring (Fig. 3a,b). More specifically, the (local) skeletal $\delta^{13}C$ minima, in cycle I as well as in cycle II, coincide with the (local) Mn/Ca maxima, which (as has been discussed earlier) coincide with (local) chlorophyll *a* maxima. Briefly, whereas primary production has been shown to give rise to an increase in $\delta^{13}C$ of the DIC (Mook, 1970; Mook and Tan, 1991; Hellings et al., 1999a,b), chlorophyll *a* maxima are, at least in the present study, associated with a decrease in skeletal $\delta^{13}C$.

The (inferred) disequilibrium between *M. edulis* shell $\delta^{13}C$ and $\delta^{13}C_{DIC}$ could be the result of a kinetic effect, causing a decrease in the incorporation of ^{13}C into the shell at higher precipitation rates (Turner, 1982; McConnaughey, 1989a; McConnaughey, 1989b). In shell formed after transplantation (Fig. 3b, cycle II), the $\delta^{13}C$ minimum does indeed coincide with the period of fastest shell growth (i.e., the first 10 weeks after transplantation; see earlier, 3.1.). These observations might be indicative of a kinetic control on the skeletal C isotope fractionation. However, according to McConnaughey (1989a,b), kinetic isotope effects usually produce linear correlations between skeletal $\delta^{13}C$ and $\delta^{18}O$. This is obviously not the case in the present study (Fig. 3a,b). Moreover, Klein et al. (1996b) found no significant correlation between within-shell variations of skeletal $\delta^{13}C$ and shell growth rate for *M. trossulus*.

The disequilibrium between shell $\delta^{13}C$ and $\delta^{13}C_{DIC}$ could also be caused by a metabolic effect, i.e., a decrease in skeletal ^{13}C due to a dilution of seawater DIC with isotopically light CO_2 derived from respiration. Tanaka et al. (1986) showed that a significant proportion (up to 85%) of mollusc shell carbon originates from metabolic carbon. Consequently, skeletal $\delta^{13}C$ variations might be primarily caused by seasonal variations in the metabolic rate, thus completely obscuring the C isotopic trend of the DIC. This is illustrated by Klein et al. (1996b) who found that $\delta^{13}C$ variations within the calcite shell layer of *M. trossulus* correlated well with salinity variations (the latter assumed to reflect variations in $\delta^{13}C_{DIC}$) in one individual, but not in another one. Klein et al. suggested that this difference might be due to a difference in metabolic (respiration) rate. If we assume that the $\delta^{13}C$ variations in the present study are indeed governed by variations in metabolic rate, the occurrence of the $\delta^{13}C$ minima in spring (in cycle I as well as cycle II; Fig. 3a,b) indicates that respiration rate is maximal during this period. Smaal et al. (1997) indeed showed that the respiration rate of *M. edulis* exhibits a clear seasonal cycle with maximal values in May. According to Smaal, these variations follow the reproductive cycle of the mussel, with respiration rate increasing during the reproductive period (March–May) and decreasing after spawning. Moreover, in the present study, skeletal $\delta^{13}C$ minima coincide with periods where chlorophyll *a* concentrations, and thus presumably food availability are maximal (see earlier). It seems likely that such periods of high food availability are associated with increases in the respiration rate of the mussels and thus with decreases in skeletal ^{13}C. $\delta^{13}C$ is lower in shell formed after transplantation than in shell deposited before transplantation. This could result from a difference in isotopic signature between the particulate organic matter in the OS and WS (Laane et al., 1990; Middelburg and Nieuwenhuize, 1998). Alternately, the mussel's metabolic rate in the WS might have been higher than in the OS as a result of differences in food availability (see chlorophyll *a* data in discussion on Ba). A possible decrease in metabolic activity might also be related to the ageing of the mussel (Krantz et al., 1987).

5. CONCLUSIONS

LA-ICP-MS analysis of the calcite shell layer of *M. edulis* has shown that Mg, Mn, Sr, Ba, and Pb exhibit cyclic variations that have an annual periodicity. Both environmental and physiological factors appear to have an influence on the incorporation of these trace elements into the shell.

The overall seasonal Mg, Sr, and Pb variations show great similarity. The global Mg variations cannot be explained by variations in seawater chemistry. Furthermore, a constant Mg temperature relationship was not found in the present study, indicating that temperature cannot be the sole factor controlling the incorporation of Mg into the shell. Clearly, this hampers the direct use of Mg in *M. edulis* calcite as a high resolution temperature proxy. Processes other than variations in seawater chemistry and temperature must be responsible for the global skeletal Sr variations. Similarly, preliminary findings indicate that the overall skeletal Pb trends may not be related to variations in aquatic Pb concentrations. This should be taken into account when attempting to use skeletal Pb for documenting aquatic Pb pollution.

The annual skeletal Ba and Mn maxima coincide with algal biomass maxima and presumably reflect elevated concentrations of particulate Ba and Mn associated with the phytoplankton bloom. Whereas the Ba peak is quite narrow and provides an excellent marker for the spring phytoplankton bloom, the Mn peak extends over a longer period. We propose that the Ba and Mn peaks may each be associated with the occurrence of specific types of phytoplankton.

Acknowledgments—We thank Henk Van De Bos (Zeevisserij-inspectie, The Netherlands) for providing the mussels for the transplantation experiment, Frans Van Balen and K. Saman (Ministerie van Verkeer en Waterstaat, Directoraat-Generaal Rijkswaterstaat, Directie Zeeland/Hydrometeostation, The Netherlands) for providing the temperature/salinity data and Koen Parmentier for providing the Pb concentrations. The primary productivity data were obtained from the MWTL monitoring programs of the «Ministerie van Verkeer en Waterstaat, Directoraat-Generaal Rijkswaterstaat, Rijksinstituut voor Kust en Zee

(RIKZ)», The Netherlands. We also express our gratitude to Jacques Navez for the technical support during the LA-ICP-MS analyses, to Jef Nijs for extracting the samples for isotopic analysis and to Luc André and the staff of the «Centre d'Analyse par Microsonde pour les Sciences de la Terre», Université Catholique de Louvain-la-Neuve, for the use of the electron microprobe and for the technical support during the analyses. Furthermore, we thank Philippe Willenz (Koninklijk Belgisch Instituut voor Natuurwetenschappen, Brussels) for the use of his diamond saw. The quality of this manuscript was greatly improved by the insightful comments of J. Middelburg and H. Stecher. Frank Dehairs and Erika Vander Putten are respectively Senior Research Associate and Research Assistant at the Fund for Scientific Research, Flanders (F.W.O.-Vlaanderen, Belgium).

REFERENCES

Baeyens W., Elskens M., Gillain G., and Goeyens L. (1998a) Biogeochemical behaviour of Cd, Cu, Pb and Zn in the Scheldt estuary during the period 1981–1983. In *Trace Metals in the Westerschelde Estuary: A Case-Study of a Polluted, Partially Anoxic Estuary.* (ed. W. F. J. Baeyens); *Developments in Hydrobiology* **Vol. 128,** pp. 15–44. Kluwer Academic Publishers.

Baeyens W., van Eck B., Lambert C., Wollast R., and Goeyens L. (1998b) General description of the Scheldt estuary. In *Trace Metals in the Westerschelde Estuary: A Case-Study of a Polluted, Partially Anoxic Estuary* (ed. W. F. J. Baeyens); *Developments in Hydrobiology* **Vol. 128,** pp. 1–14. Kluwer Academic Publishers.

Beliaeff B., O'Connor T. P., Daskalakis D. K., and Smith P. J. (1997) U. S. Mussel Watch Data from 1986 to 1994: Temporal Trend Detection at Large Spatial Scales. *Environ. Sci. Technol.* **31,** 1411–1415.

Bishop J. K. B. (1988) The barite–opal–organic carbon association in oceanic particulate matter. *Nature* **332,** 341–343.

Bourgoin B. P. (1990) Mytilus edulis shell as a bioindicator of lead pollution: Considerations on bioavailability and variability. *Mar. Ecol. Prog. Ser.* **61,** 253–262.

Carpenter S. J. and Lohmann K. C. (1992) Sr/Mg ratios of modern marine calcite: Empirical indicators of ocean chemistry and precipitation rate. *Geochim. Cosmochim. Acta* **56,** 1837–1849.

Chow T. J. and Goldberg E. D. (1960) On the marine geochemistry of barium. *Geochim. Cosmochim. Acta* **20,** 192–198.

Coplen T. B. (1994) Reporting of stable hydrogen, carbon and oxygen isotopic abundances. *Pure Appl. Chem.* **66,** 273–276.

Crenshaw M. A. (1972) The inorganic composition of molluscan extrapallial fluid. *Biol. Bull.* **143,** 506–512.

Dehairs F., Chesselet R., and Jedwab J. (1980) Discrete suspended particles of barite and the barium cycle in the open ocean. *Earth Planet. Sci. Lett.* **49,** 528–550.

Dehairs F., Lambert C. E., Chesselet R., and Risler N. (1987) The biological production of marine suspended barite and the barium cycle in the Western Mediterranean Ocean. *Biogeochemistry* **4,** 119–139.

Dodd J. R. (1965) Environmental control of strontium and magnesium in *Mytilus. Geochim. Cosmochim. Acta* **29,** 385–398.

Dodd J. R. and Crisp E. L. (1982) Non-linear variation with salinity of Sr/Ca and Mg/Ca ratios in water and aragonitic bivalve shells and implications for palaeosalinity studies. *Palaeogeogr., Palaeoclim., Palaeoecol.* **38,** 45–56.

Donner J. and Nord A. G. (1986) Carbon and oxygen stable isotope values in shells of *Mytilus edulis* and *Modiolus modiolus* from Holocene raised beaches at the outer coast of the Varanger Peninsula, North Norway. *Palaeogeogr., Palaeoclim., Palaeoecol.* **56,** 35–50.

Epstein S., Bushbaum R., Lowenstam H., and Urey H.C. (1953) Revised carbonate-water isotopic temperature scale. *Geol. Soc. Amer. Bull.* **62,** 417–426.

Fritz L. W., Ragone L. M., and Lutz R. A. (1990) Biomineralization of barite in the shell of the freshwater Asiatic clam *Corbicula fluminea* (Mollusca: Bivalvia). *Limnol. Oceanogr.* **35,** 756–762.

Fuge R., Palmer T. J., Pearce N. J. G., and Perkins W. T. (1993) Minor and trace element chemistry of modern shells: A laser ablation inductively coupled plasma mass spectrometry study. *Appl. Geochem.* **Suppl. Issue No 2,** 111–116.

Goldberg E. D. and Arrhenius G. O. S. (1958) Chemistry of Pacific pelagic sediments. *Geochim. Cosmochim. Acta* **13,** 153–212.

Goldsmith J. R., Graf D. L., and Heard H. C. (1961) Lattice constants of the calcium magnesium carbonates. *Am. Mineral.* **46,** 453–457.

Gossling E. M. (1992) Systematics and geographic distribution of *Mytilus*. In *The mussel Mytilus: Ecology, Physiology, Genetics and Culture* (ed. E. M. Gossling); *Developments in Aquaculture and Fisheries Science.* **Vol. 25,** Ch. 1, pp. 1–20. Elsevier.

Hart S. R. and Blusztajn J. (1998) Clams as Rcorders of Ocean Ridge Volcanism and Hydrothermal Vent Field Activity. *Science* **280,** 883–886.

Hartley G. and Mucci A. (1996) The influence of P_{CO2} on the partitioning of magnesium in calcite overgrowths precipitated from artificial seawater at 25°C and 1 atm total pressure. *Geochim. Cosmochim. Acta* **60,** 315–324.

Hellings L., Dehairs F., and Baeyens, W. (1999a) Origin and fate of dissolved inorganic carbon in the brackish and freshwater part of a highly polluted European estuary. Submitted to *Limnol. Oceanogr.*

Hellings L., Dehairs F., Tackx M., Keppens E., and Baeyens, W. (1999b) Origin and fate of organic carbon in the freshwater part of the Scheldt Estuary as traced by stable carbon isotope composition. *Biogeochemistry* **47,** 167–186.

Klein R. T., Lohmann K. C., and Thayer C. W. (1996a) Bivalve skeletons record seas-surface temperature and $\delta^{18}O$ via Mg/Ca and $^{18}O/^{16}O$ ratios. *Geology* **24,** 415–418.

Klein R. T., Lohmann K. C., and Thayer C. W. (1996b) Sr/Ca and $^{13}C/^{12}C$ ratios in skeletal calcite of *Mytilus trossulus*: Covariation with metabolic rate, salinity, and carbon isotopic composition of seawater. *Geochim. Cosmochim. Acta* **60,** 4207–4221.

Krantz D. E., Williams D. F., and Jones D. S. (1987) Ecological and paleoenvironmental information using stable isotopes from living and fossil molluscs. *Palaeogeogr., Palaeoclim., Palaeoecol.* **58,** 249–266.

Laane R. W. P. M., Turkstra E., and Mook W. G. (1990) Stable Carbon Isotope Composition of Pelagic and Benthic Organic Matter in the North Sea and Adjacent Estuaries. In *Facts of Modern Biogeochemistry: Festschrift for E. T. Degens* (ed. V. Ittekot, S. Kempe, W. Michaelis, A. Spitzy), pp. 214–224.

Lancelot C. (1984) Metabolic changes in Phaeocystis pouchetii (Hariot) Lagerheim during the spring bloom in Belgian coastal waters. *Estuar. Coastal Shelf Sci.* **18,** 593–600.

Lingard S. M., Evans R. D., and Bourgoin B. P. (1992) Method for the Estimation of Organic-Bound and Crystal-Bound Metal Concentrations in Bivalve Shells. *Bull. Environ. Contam. Toxicol.* **48,** 179–184.

Lorens R. B. (1981) Sr, Cd, Mn and Co distribution coefficients in calcite as a function of calcite precipitation rate. *Geochim. Cosmochim. Acta* **45,** 553–561.

Lorens R. B. and Bender M. L. (1980) The impact of solution chemistry on *Mytilus edulis* calcite and aragonite. *Geochim. Cosmochim. Acta* **44,** 1265–1278.

Lubbers G. W., Gieskes W. W. C., del Castilho P., Salomons W., and Bril J. (1990) Manganese accumulation in the high pH microenvironment of *Phaeocystis* sp. (Haptophyceae) colonies from the North Sea. *Mar. Ecol. Prog. Series* **59,** 285–293.

McConnaughey T. (1989a) ^{13}C and ^{18}O isotopic disequilibrium in biological carbonates: I. Patterns. *Geochim. Cosmochim. Acta* **53,** 151–162.

McConnaughey T. (1989b) ^{13}C and ^{18}O isotopic disequilibrium in biological carbonates: II. In vitro simulation of kinetic isotope effects. *Geochim. Cosmochim. Acta* **53,** 163–171.

Middelburg J. J. and Nieuwenhuize J. (1998) Carbon and nitrogen stable isotopes in suspended matter and sediments from the Schelde Estuary. *Mar. Chem.* **60,** 217–225.

Mook W. G. (1970) Stable carbon and oxygen isotopes of natural waters in the Netherlands. In *Proceedings IAEA Conference on Isotopes in Hydrology, Vienna,* pp. 163–190.

Mook W. G. (1971) Paleotemperatures and chlorinities from stable carbon and oxygen isotopes in shell carbonate. *Palaeogeogr., Palaeoclim., Palaeoecol.* **9,** 245–263.

Mook W. G. and Tan F. C. (1991) Stable Carbon Isotopes in Rivers and Estuaries. In *Biogeochemistry of Major World Rivers* (ed. E. T.

Degens, S. Keme and J. E. Richey), pp. 245–264. John Wiley and Sons.

Morris A. W. (1971) Trace metal variations in sea water of the Menai Straits caused by a bloom of *Phaeocystis. Nature, Lond.* **233,** 427–428.

Morse J. W. and Mucci A. (1984) Composition of carbonate overgrowths produced in Iceland Spar calcite crystals buried in Bahamian carbonate-rich sediments. *Sed. Geol.* **40,** 287–291.

Mucci A. and Morse J. W. (1983) The incorporation of Mg^{2+} and Sr^{2+} into calcite overgrowths: influences of growth rate and solution composition. *Geochim. Cosmochim. Acta* **47,** 217–233.

Nienhuis P. H. and Smaal A. C. (1994) The Oosterschelde estuary, a case-study of a changing ecosystem: an introduction. In *The Oosterschelde Estuary (The Netherlands): A Case-Study of a Changing Ecosystem* (ed. P. H. Nienhuis and A. C. Smaal); *Developments in Hydrobiology*. **Vol. 97,** pp. 1–14. Kluwer Academic Publishers.

Pearce N.J.G., Perkins W. T., Westgate J. A., Gorton M. P., Jackson S. E., Neal C. R., and Chenery S. P. (1997) A Compilation of New and Published Major and Trace Element Data for NIST SRM 610 and NIST SRM 612 Glass Reference Materials. *Geostand. Newsl.* **21,** 115–144.

Perkins W. T. and Pearce N. J. G. (1995) Mineral microanalysis by laserprobe inductively coupled plasma mass spectrometry. In *Microprobe Tehniques in the Earth Sciences* (ed. P. J. Potts, J. F. W. Bowles, S. J. B. Reed, and M. R. Cave); Chap. 7, pp. 289–325, Chapman and Hall, London.

Pitts L. C. and Wallace G. T. (1994) Lead deposition in the Shell of the Bivalve, Mya arenaria: An indicator of Dissolved Lead in Seawater. *Estuar. Coastal Shelf Sci.* **39,** 93–104.

Price G. D. and Pearce N. J. G. (1997) Biomonitoring of pollution by *Cerastoderma edule* from the British Isles: A Laser Ablation ICP-MS study. *Mar. Poll. Bull.* **34,** 1025–1031.

Raith A., Perkins W. T., Pearce N. J. G., and Jeffries T. E. (1996) Environmental monitoring on shellfish using UV laser ablation ICP-MS. *Fresenius J. Anal. Chem.* **355,** 789–792.

Reeder R. J. and Grams C. J. (1987) Sector zoning in calcite cement crystals: Implications for trace element distribution coefficients in carbonates. *Geochim. Cosmochim. Acta* **51,** 187–194.

Reeder R. J. and Paquette J. (1989) Sector zoning in natural and synthetic calcites. *Sed. Geol.* **65,** 239–247.

Reeder R. J. and Prosky J. L. (1986) Compositional sector zoning in dolomite. *J. Sediment. Petrol.* **56,** 237–247.

Richardson L. L. and Stolzenbach K. D. (1995) Phytoplankton cell size and the development of microenvironments. *FEMS Microb. Ecol.* **16,** 185–192.

Richardson L. L., Aguilar C., and Nealson K. H. (1988) Manganese oxidation in pH and O_2 microenvironments produced by phytoplankton. *Limnol. Oceanogr.* **33,** 352–363.

Rosenberg G. D. and Hughes W. W. (1991) A metabolic model for the determination of shell composition in the bivalve mollusc, *Mytilus edulis. Lethaia* **24,** 83–96.

Schettler G. and Pearce N. J. G. (1996) Metal pollution in extinct *Dreissena polymorpha* communities, Lake Breitling, Havel Lakes system, Germany: A laser ablation inductively coupled plasma mass spectrometry study. *Hydrobiologia* **317,** 1–11.

Seed R. and Suchanek T. H. (1992) Population and community ecology of *Mytilus.* In *The mussel Mytilus: Ecology, Physiology, Genetics and Culture* (ed. E. M. Gossling); *Developments in Aquaculture and Fisheries Science.* **Vol. 25,** Chap. 4, pp. 87–170. Elsevier.

Smaal A. C., Vonck A. P. M. A., and Bakker M. (1997) Seasonal variation in physiological energetics of *Mytilus edulis* and *Cerastoderma edule* of different size classes. *J. Mar. Biol. Ass. U.K.* **77,** 817–838.

Stecher H. A. III, Krantz D. E., Lord C. J. III, Luther G. W. III, and Bock K. W. (1996) Profiles of strontium and barium in *Mercenaria mercenaria* and *Spisula solidissima* shells. *Geochim. Cosmochim. Acta* **60,** 3445–3456.

Stroobants N., Dehairs F., Goeyens L., Vanderheijden N., and Van Grieken R. (1991) Barite formation in the Southern Ocean water column. *Mar. Chem.* **35,** 411–421.

Sunda W. G. and Huntsman S. A. (1985) Regulation of cellular manganese and manganese transport rates in the unicellular alga *Chlamydomonas. Limnol. Oceanogr.* **30,** 71–80.

Sunda W. G. and Huntsman S. A. (1988) Effect of sunlight on redox cycles of manganese in the southwestern Sargasso Sea. *Deep Sea Res. Part A Oceanogr. Res. Pap.* **35,** 1297–1318.

Tanaka N., Monaghan M. C., and Rye D. M. (1986) Contribution of metabolic carbon to mollusc and barnacle shell carbonate. *Nature* **320,** 520–523.

Turner J. V. (1982) Kinetic fractionation of carbon-13 during calcium carbonate precipitation. *Geochim. Cosmochim. Acta* **46,** 1183–1191.

Valenta P., Duursma E. K., Merks A. G. A., Rutzel H., and Nurnberg H. W. (1986) Distribution of Cd, Pb and Cubetween the dissolved phase and the particulate phase in the Eastern Scheldt and the Western Scheldt Estuary. *Sci. Tot. Envir.* **53,** 41–76.

Vander Putten E., Dehairs F., André L., and Baeyens W. (1999) Quantitative in situ microanalysis of minor and trace elements in biogenic calcite using infrared laser ablation-inductively coupled plasma mass spectrometry: A critical evaluation. *Anal. Chim. Acta* **378,** 261–272.

Wilbur K. M. and Saleuddin A. S. M. (1983) Shell Formation. In *The Mollusca* (ed. A. S. M. Saleuddin and K. M. Wilbur), pp. 236–279. Acad. Press.